Journal of Sound and Vibration (1999) **221**(3), 491–503
Article No. jsvi.1998.2003, available online at http://www.idealibrary.com on IDEAL

NON-LINEAR VIBRATIONS OF A BEAM–MASS SYSTEM WITH BOTH ENDS CLAMPED

E. Özkaya and M. Pakdemirli

Department of Mechanical Engineering, *Celal Bayar University*, 45140 *Muradiye*, *Manisa*, *Turkey*

(*Received* 27 *July* 1998, *and in final form* 8 *October* 1998)

A clamped–clamped beam–mass system is considered. The non-linear equations of motion including stretching due to immovable end conditions were derived previously [1] (Özkaya *et al*. 1997 *Journal of Sound and Vibration* **199**, 679–696). In addition to five different end conditions considered in reference [1], the case of clamped–clamped edge conditions is treated in this work. Exact solutions for the mode shapes and frequencies are given for the linear part of the problem. For the non-linear problem, approximate solutions using perturbations are searched. Alternatively, the natural frequencies and non-linear corrections are used in training a multi-layer, feed-forward, back propagation artificial neural network (ANN) algorithm. Using the algorithm, the numerical calculations are drastically reduced for obtaining the natural frequencies and non-linear corrections corresponding to different input parameters.

1. INTRODUCTION

Non-linear vibrations of beams are extensively studied. One type of non-linearity, which arises when immovable end conditions are used, is due to the stretching of the beam itself. The work on this type of non-linearity is reviewed up to 1979 by Nayfeh and Mook [2]. More recent works on the topic are due to Hou and Yuan [3], McDonald [4], Pakdemirli and Nayfeh [5], Özkaya *et al*. [1] and Karlik *et al*. [6]. For slightly curved beams with stretching, one may refer to Rehfield [7] and Öz *et al*. [8]. For centre load beams, Low *et al*. [9] found that the results of experiments and the theory did not match well for beams of large slenderness ratio. In a later paper [10], when stretching effects were included, the correlation between theory and experiments was much improved.

Finally, for linear vibrations of beam–mass systems, detailed calculations for fundamental frequencies as well as comparisons with exact values given in reference [1] can be found in references [11–14].

The analysis presented here is closely related to references [1] and [6]. In reference [1], five different immovable end conditions are treated. However, the case of clamped–clamped edge conditions is not considered in that reference. In this work, exact mode shapes and frequencies are calculated for clamped–clamped edge conditions of a beam–mass system. Following reference [1], the amplitude

0022–460X/99/130491 + 13 $30.00/0

dependent non-linear frequencies are found approximately using the method of multiple scales, a perturbation technique. Forced vibrations are also treated and frequency response curves are drawn. Then, similar to the analysis given in reference [6], a back propagation, feed forward, multi-layer artificial neural network (ANN) algorithm is trained using exact natural frequency values and non-linear correction coefficients. For the linear part, the input parameters are α (ratio of concentrated mass to beam mass) and η (concentrated mass location) and the output are the first five natural frequencies. For the non-linear part, only the fundamental frequency is considered and with the same input parameters, the non-linear correction coefficient (λ) is calculated. Results show that ANN algorithm can be used within reasonable accuracy in order to decrease computational time.

2. EQUATIONS OF MOTION

The system considered is a beam of length L clamped at both ends. A concentrated mass M is located at position $x = x_s$ where x is the spatial co-ordinate along the beam (Figure 1).

The dimensionless equations of motion and boundary conditions for the problem were derived using Hamilton's principle [5, 1],

$$\ddot{w}_1 + w_1^{iv} = (1/2)\left[\int_0^\eta w_1'^2\,\mathrm{d}x + \int_\eta^1 w_2'^2\,\mathrm{d}x\right]w_1'' - 2\bar{\mu}\dot{w}_1 + \overline{F}_1\cos\Omega t, \tag{1}$$

$$\ddot{w}_2 + w_2^{iv} = (1/2)\left[\int_0^\eta w_1'^2\,\mathrm{d}x + \int_\eta^1 w_2'^2\,\mathrm{d}x\right]w_2'' - 2\bar{\mu}\dot{w}_2 + \overline{F}_2\cos\Omega t, \tag{2}$$

$$w_1(0, t) = w_1'(0, t) = w_2(1, t) = w_2'(1, t) = 0, \tag{3}$$

$$w_1(\eta, t) = w_2(\eta, t), \qquad w_1'(\eta, t) = w_2'(\eta, t), \qquad w_1''(\eta, t) = w_2''(\eta, t), \tag{4}$$

$$w_1'''(\eta, t) - w_2'''(\eta, t) - \alpha\ddot{w}_1(\eta, t) = 0, \tag{5}$$

where w_1 and w_2 are the left and right transverse displacements with respect to the concentrated mass M. $(\dot{\ })$ denotes differentiation with respect to dimensionless time t and $(\ )'$ denotes differentiation with respect to dimensionless spatial variable x. $\bar{\mu}$ is the viscous damping coefficient, $\overline{F}_1$ and Ω are the external excitation amplitude

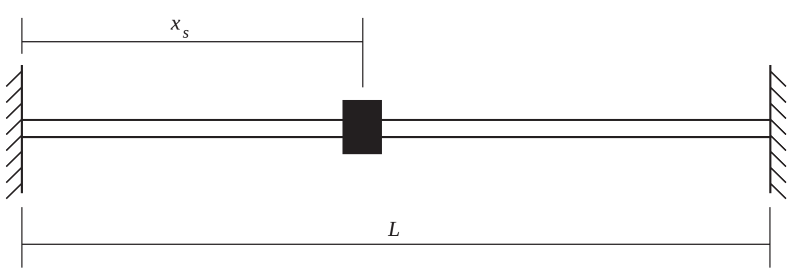

Figure 1. Beam–mass system with both ends clamped.

and frequency respectively. η is the dimensionless mass location ($0 < \eta < 1$). The dimensional (denoted by asterisk) and dimensionless quantities are related through the following equations

$$x = x^*/L, \qquad w_{1,2} = w^*_{1,2}/r, \qquad \eta = x_s/L,$$
$$t = (1/L^2)(EI/\rho A)^{1/2} t^*, \qquad \alpha = M/\rho AL,$$
$$\Omega = \Omega^* L^2/(EI/\rho A)^{1/2}, \qquad \bar{F}_{1,2} = F^*_{1,2}/EIr, \qquad 2\bar{\mu} = (\mu^* L^2)/(\rho AEI)^{1/2}, \tag{6}$$

where r is the radius of gyration of the beam cross-section with respect to the neural axis and I its moment of inertia, ρ denotes the density of the beam and A the area of the cross-section and E Young's modulus. α is the ratio of the concentrated mass to the beam mass.

3. APPROXIMATE ANALYTICAL SOLUTIONS

Following reference [1], an approximate expansion of the form is assumed

$$w_1(x, t; \varepsilon) = \varepsilon w_{11}(x, T_0, T_2) + \varepsilon^3 w_{13}(x, T_0, T_2) + \ldots, \tag{7}$$

$$w_2(x, t; \varepsilon) = \varepsilon w_{21}(x, T_0, T_2) + \varepsilon^3 w_{23}(x, T_0, T_2) + \ldots, \tag{8}$$

where ε is the perturbation parameter and $T_0 = t$ and $T_2 = \varepsilon^2 t$ are the usual slow and fast time scales in the method of multiple scales. Re-ordering the damping and excitation, defining the time derivatives in terms of T_0 and T_2

$$\bar{\mu} = \varepsilon^2 \mu, \qquad \bar{F}_{1,2} = \varepsilon^3 F_{1,2},$$
$$(\dot{\ }) = D_0 + \varepsilon^2 D_2, \qquad (\ddot{\ }) = D_0^2 + 2\varepsilon^2 D_0 D_2, \qquad D_n = \partial/\partial T_n, \tag{9}$$

and substituting all into the partial differential system (1)–(5) yields

Order ε:

$$D_0^2 w_{11} + w_{11}^{iv} = 0, \qquad D_0^2 w_{21} + w_{21}^{iv} = 0, \tag{10}$$

$$w_{11} = w'_{11} = 0 \quad \text{at} \quad x = 0, \qquad w_{21} = w'_{21} = 0 \quad \text{at} \quad x = 1, \tag{11}$$

$$w_{11} = w_{21}, \qquad w'_{11} = w'_{21}, \qquad w''_{11} = w''_{21}, \qquad w'''_{11} - w'''_{21} - \alpha D_0^2 w_{11} = 0 \quad \text{at} \quad x = \eta. \tag{12}$$

Order ε^3:

$$D_0^2 w_{13} + w_{13}^{iv} = -2D_0 D_2 w_{11} - 2\mu D_0 w_{11} + (1/2)\left[\int_0^\eta w'^2_{11}\,\mathrm{d}x + \int_\eta^1 w'^2_{21}\,\mathrm{d}x\right] w''_{11} + F_1 \cos \Omega T_0, \tag{13}$$

$$D_0^2 w_{23} + w_{23}^{iv} = -2D_0 D_2 w_{21} - 2\mu D_0 w_{21} + (1/2)\left[\int_0^\eta w'^2_{11}\,\mathrm{d}x + \int_\eta^1 w'^2_{21}\,\mathrm{d}x\right] w''_{21} + F_2 \cos \Omega T_0, \tag{14}$$

$$w_{13} = w'_{13} = 0 \quad \text{at} \quad x = 0, \qquad w_{23} = w'_{23} = 0 \quad \text{at} \quad x = 1, \tag{15}$$

$$w_{13} = w_{23}, \qquad w'_{13} = w'_{23}, \qquad w''_{13} = w''_{23},$$
$$w'''_{13} - w'''_{23} - \alpha D_0^2 w_{13} - 2\alpha D_0 D_2 w_{11} = 0 \quad \text{at} \quad x = \eta. \tag{16}$$

3.1. EXACT SOLUTION TO THE LINEAR PROBLEM

The linear problem is governed by equations (10)–(12). Assuming solutions of the form

$$w_{11} = [A(T_2)\,\mathrm{e}^{\mathrm{i}\omega T_0} + cc]Y_1(x), \qquad w_{21} = [A(T_2)\,\mathrm{e}^{\mathrm{i}\omega T_0} + cc]Y_2(x), \tag{17}$$

and substituting into equations (10)–(12), one obtains

$$Y_1^{iv} - \omega^2 Y_1 = 0, \qquad Y_2^{iv} - \omega^2 Y_2 = 0, \tag{18}$$

$$Y_1(0) = Y'_1(0) = Y_2(1) = Y'_2(1) = 0, \tag{19}$$

$$Y_1(\eta) = Y_2(\eta), \qquad Y'_1(\eta) = Y'_2(\eta), \qquad Y''_1(\eta) = Y''_2(\eta), \tag{20}$$

$$Y'''_1(\eta) - Y'''_2(\eta) + \alpha\omega^2 Y_1(\eta) = 0. \tag{21}$$

Exact solutions for the mode shapes (Y_1, Y_2) and frequencies (ω) are available for the system (18)–(21). The mode shapes are found to be

$$\begin{aligned} Y_1(x) = C\{&(\cosh\beta(1-\eta)\sin\beta - \sin\beta\eta - \cosh\beta\sin\beta(1-\eta) \\ &+ \cos\beta(1-\eta)\sinh\beta - \sinh\beta\eta \\ &- \cos\beta\sinh\beta(1-\eta))(\cos\beta x - \cosh\beta x) \\ &- (-\cos\beta\eta + \cos\beta(1-\eta)\cosh\beta - \cosh\beta\eta \\ &+ \cos\beta\cosh\beta(1-\eta) - \sin\beta(1-\eta)\sinh\beta \\ &+ \sin\beta\sinh\beta(1-\eta))(\sin\beta x - \sinh\beta x)\}, \end{aligned} \tag{22}$$

$$\begin{aligned} Y_2(x) = C\{&\sin\beta x(-\cos\beta\eta + \cos\beta(1+\eta)\cosh\beta + \cosh\beta\eta \\ &- \cos\beta\cosh\beta(1-\eta) \\ &+ \sin\beta(1-\eta)\sinh\beta - \sin\beta\sinh\beta(1-\eta)) \\ &+ \cosh\beta x(-(\cosh\beta\sin\beta) + \cos\beta\sinh\beta) \\ &\times(-\cos\beta\eta + \cos\beta(1+\eta)\cosh\beta + \cosh\beta\eta \\ &- \cos\beta\cosh\beta(1-\eta) + \sin\beta(1-\eta)\sinh\beta \\ &- \sin\beta\sinh\beta(1-\eta) + (-(\cos\beta\cosh\beta) \\ &+ \sin\beta\sinh\beta)(-\cos\beta\eta + \cos\beta(1+\eta)\cosh\beta \\ &+ \cosh\beta\eta - \cos\beta\cosh\beta(1-\eta) + \sin\beta(1-\eta)\sinh\beta \\ &- \sin\beta\sinh\beta(1-\eta))\sinh\beta x \\ &+ \cosh\beta(1-\eta)\sin\beta + \sin\beta\eta - \cosh\beta\sin\beta(1+\eta) \\ &+ \cos\beta(1-\eta)\sinh\beta - \sinh\beta\eta \\ &- \cos\beta\sinh\beta(1-\eta))(\cos\beta x - \cos\beta\cosh\beta(1-x) \\ &- \sin\beta\sinh\beta(1-x))\}, \end{aligned} \tag{23}$$

where β are the square root of the natural frequencies

$$\beta = \sqrt{\omega}. \tag{24}$$

The transcendental equation giving β values and hence the natural frequencies is

$$\begin{aligned}4 &- 4\cos\beta\cosh\beta + \alpha\beta\cosh\beta\sin\beta + \alpha\beta\cosh\beta(1-2\eta)\sin\beta\\ &- 2\alpha\beta\cosh\beta\eta\sin\beta\eta - 2\alpha\beta\cosh\beta(1-\eta)\sin\beta(1-\eta)\\ &- \alpha\beta\cos\beta\sinh\beta - \alpha\beta\cos\beta(1-2\eta)\sinh\beta\\ &+2\alpha\beta\cos\beta\eta\sinh\beta\eta + 2\alpha\beta\cos\beta(1-\eta)\sinh\beta(1-\eta) = 0.\end{aligned} \tag{25}$$

For the different mass ratio (α) and mass location (η) values, the first five natural frequencies are calculated exactly using the transcendental equation and are given in Table 1.

3.2. NON-LINEAR PROBLEM

At order ε^3, one obtains the non-linear corrections to the problem. At this level, a solvability condition is found (see reference [1] for details)

$$2\mathrm{i}\omega(A' + \mu A) + (3/2)b^2A^2\bar{A} + 2\alpha\mathrm{i}\omega A' Y_1^2(\eta) - (1/2)f\,\mathrm{e}^{\mathrm{i}\sigma T_2} = 0, \tag{26}$$

where σ is a detuning parameter, defined to express the nearness of excitation frequency to one of the natural frequencies through the relation

$$\Omega = \omega + \varepsilon^2\sigma. \tag{27}$$

TABLE 1

The first five natural frequencies corresponding to various α and η values

α	η	ω_1	ω_2	ω_3	ω_4	ω_5
0·1	0	22·3733	61·6728	120·9032	199·8604	298·5569
	0·1	22·3330	61·0122	117·1070	188·1314	279·0383
	0·2	21·9428	57·4582	110·4979	189·2495	294·5617
	0·3	21·0996	56·1969	117·7116	198·4802	280·0602
	0·4	20·2934	59·1127	119·0085	186·6530	298·0595
	0·5	19·9795	61·6727	112·1227	199·8604	279·0704
1	0	22·3733	61·6728	120·9032	199·8604	298·5569
	0·1	21·9474	53·8427	89·8598	151·9623	243·0824
	0·2	18·3360	40·9434	93·3305	177·8542	290·1980
	0·3	14·4030	44·2995	112·5615	195·4739	254·3674
	0·4	12·4047	53·5218	114·5992	167·6507	297·2762
	0·5	11·8182	61·6727	95·7568	199·8604	253·7298
10	0	22·3733	61·6728	120·9032	199·8604	298·5569
	0·1	16·9974	30·3912	74·1488	143·9640	237·8504
	0·2	8·1881	32·7612	89·2503	175·4671	289·2006
	0·3	5·5477	40·2350	110·0410	194·3152	248·0908
	0·4	4·5674	51·4102	112·8375	162·7538	297·0418
	0·5	4·3025	61·0727	90·2481	199·8604	247·4832

The arbitrary coefficient multiplying equations (22) and (23) is selected such that the normalizing condition holds

$$\int_0^\eta Y_1^2\,\mathrm{d}x + \int_\eta^1 Y_2^2\,\mathrm{d}x = 1. \tag{28}$$

The coefficients b and f in equation (26) are defined as

$$b = \int_0^\eta Y_1'^2\,\mathrm{d}x + \int_\eta^1 Y_2'^2\,\mathrm{d}x, \qquad f = \int_0^\eta F_1 Y_1\,\mathrm{d}x + \int_\eta^1 F_2 Y_2\,\mathrm{d}x. \tag{29}$$

The complex amplitudes A can be written in terms of a real amplitude a and an angle θ

$$A = (1/2)a(T_2)\,\mathrm{e}^{\mathrm{i}\theta(T_2)}. \tag{30}$$

For free vibrations, the non-linear frequencies can be defined as (see reference [1] for details)

$$\omega_{nl} = \omega + \lambda a_0^2, \tag{31}$$

where

$$\lambda = \frac{3b^2}{16\omega k} \tag{32}$$

and

$$k = 1 + \alpha Y_1^2(\eta). \tag{33}$$

Note that a_0 is the steady-state real amplitude of the response.

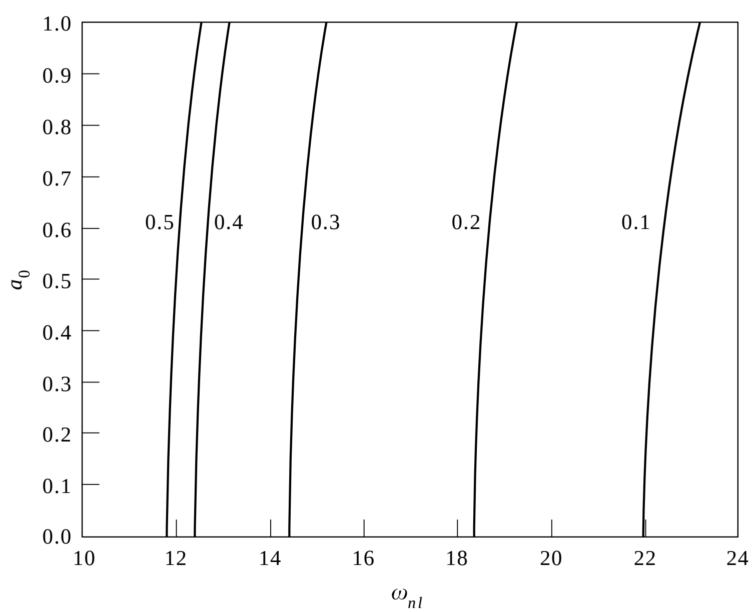

Figure 2. Non-linear frequency versus amplitude for different mass location values (first mode, $\alpha = 1$, η values are indicated on the curves).

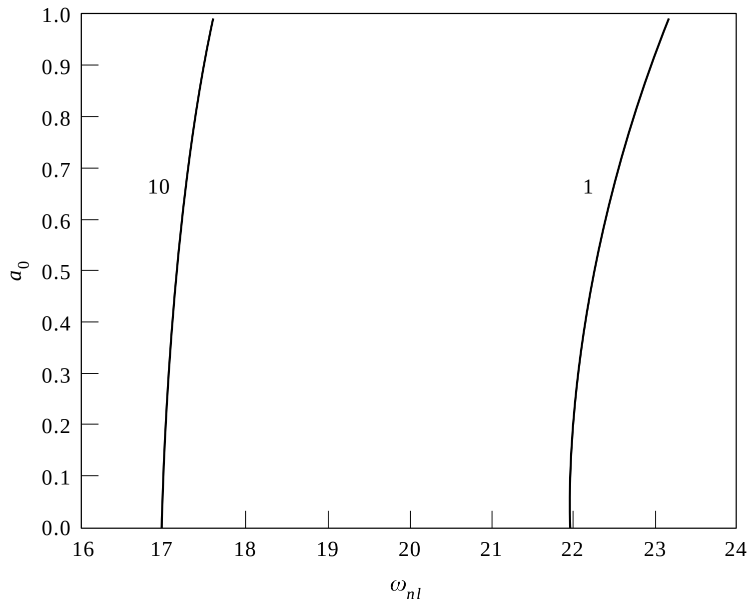

Figure 3. Non-linear frequency versus amplitude for different mass ratio values (first mode, $\eta = 0{\cdot}1$, α values are indicated on the curves).

In Figure 2, the non-linear frequencies are drawn for different mass locations. As the mass shifts to the midpoint, the linear as well as the amplitude dependent non-linear frequencies decrease for the fundamental modes. Figure 3 shows the

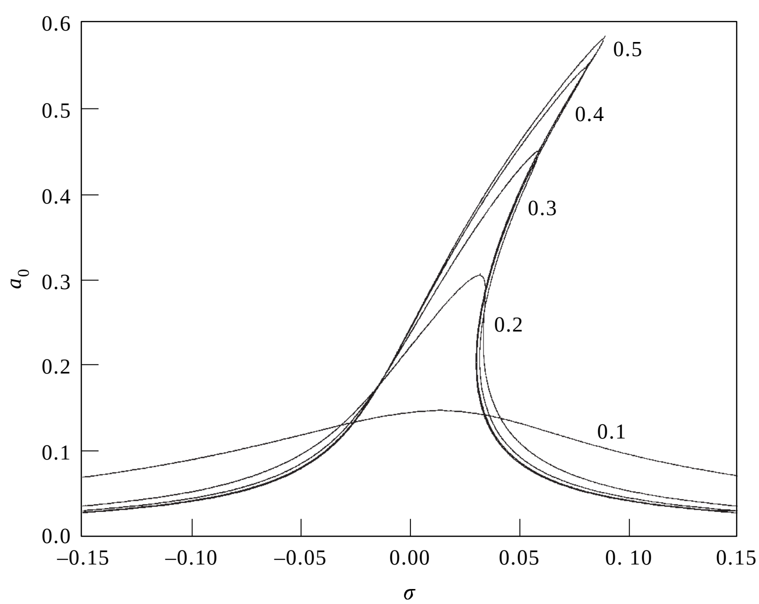

Figure 4. Frequency-response curves for different mass location (first mode, $\alpha = 10$, $\tilde{f} = 1$, $\tilde{\mu} = 0{\cdot}2$, η values are indicated on the curves).

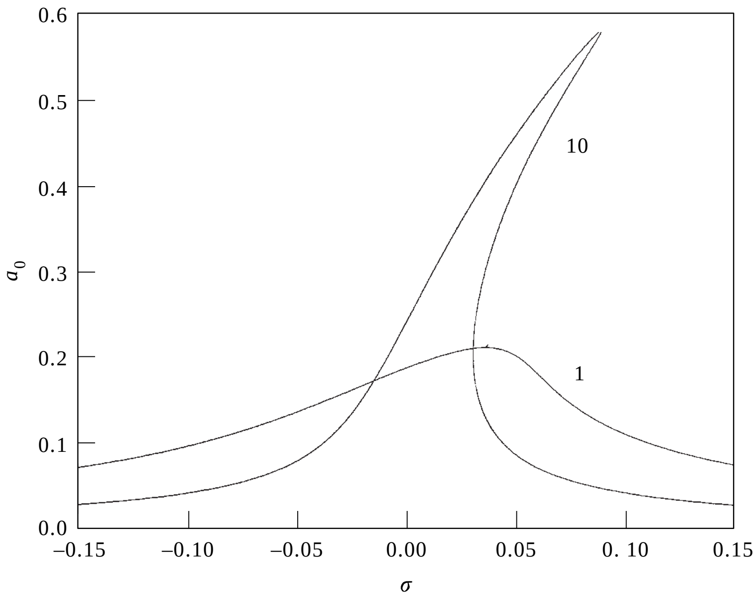

Figure 5. Frequency-response curves for different mass ratios (first mode, $\eta = 0{\cdot}5, \tilde{f} = 1, \tilde{\mu} = 0{\cdot}2$, α values are indicated on the curves).

effect of mass increase on the non-linear frequencies of the fundamental modes. As seen, an increase in concentrated mass decreses the linear and non-linear frequencies.

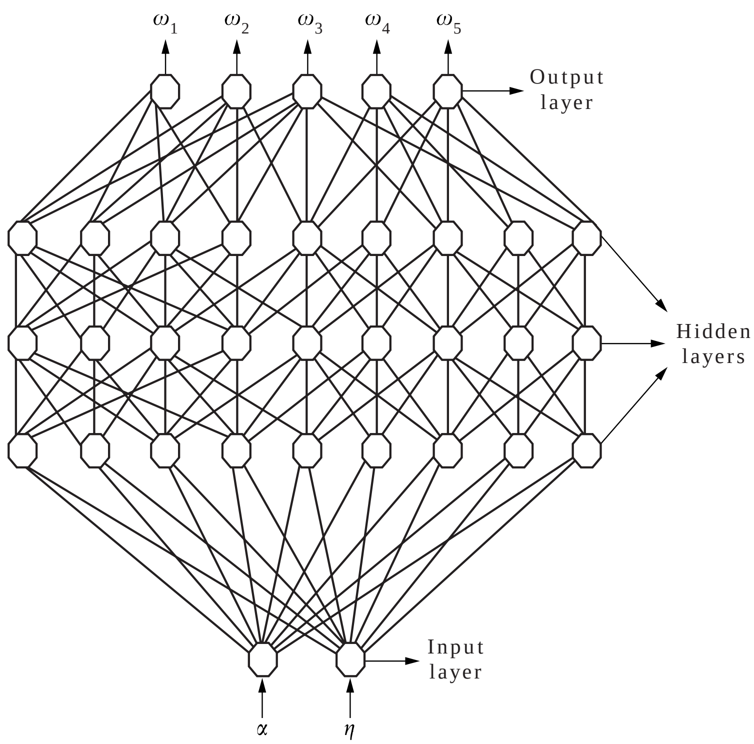

Figure 6. The ANN architecture used in the linear analysis.

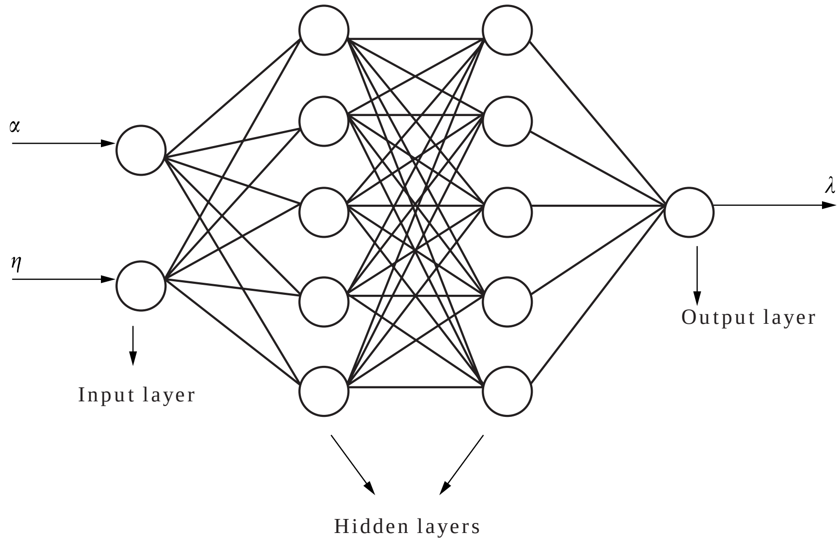

Figure 7. The ANN architecture used in the non-linear analysis.

For the forced vibrations, the steady-state frequency–response relation can be found to be [1]

$$\sigma = \lambda a^2 \mp \sqrt{\frac{\tilde{f}^2}{4\omega^2 a^2} - \tilde{\mu}^2}, \tag{34}$$

where

$$\tilde{f} = f/k, \qquad \tilde{\mu} = \mu/k. \tag{35}$$

The frequency–response curves are given for fixed mass ratio ($\alpha = 10$) and for different mass locations in Figure 4. For fixed mass location (midpoint) and varying mass ratio Figure 5 is plotted.

4. ARTIFICIAL NEURAL NETWORK APPROACH (ANN)

In this section, an alternative supplementary numerical technique of Artificial Neural Networks is used to predict the linear and non-linear frequencies. The ANN architecture is a multi-layer, feed-forward, back propagation architecture. The non-linear activation function is chosen as the sigmoid function. Details of the algorithm can be found in reference [6]. The momentum and learning rate values are taken as 0·9 and 0·7, respectively. These values are found to be optimum values by trial and error. For both the linear and non-linear parts 50 000 iterations are performed in training the algorithm. The ANN architecture used in the linear part is a 2:9:9:9:5 multi-layer architecture where α and η are the input parameters and the first five natural frequencies are the output values (Figure 6).

TABLE 2

Comparison of Newton–Raphson and ANN natural frequencies

α	η		ω_1	ω_2	ω_3	ω_4	ω_5
0·8	0·1	NR	22·0367	55·5213	93·6041	154·2763	244·5377
		ANN	22·0420	55·5030	93·5003	154·2049	244·3373
	0·2	NR	19·0622	42·6976	94·3560	178·4495	290·4400
		ANN	19·0262	42·6104	94·2475	178·3964	290·2432
	0·3	NR	15·3857	45·2185	112·9076	195·7173	255·8848
		ANN	15·3333	45·1652	113·0655	195·4040	255·5645
	0·4	NR	13·3823	53·9715	114·9766	168·8180	297·3314
		ANN	13·3215	53·9889	114·9362	168·8220	297·3030
	0·5	NR	12·7817	61·6727	96·9650	199·8604	255·2262
		ANN	12·7548	61·6402	96·8771	199·8220	254·7443
4	0·1	NR	20·3892	38·0030	76·4768	145·2097	238·7117
		ANN	20·3762	37·9298	76·3950	145·0330	238·6074
	0·2	NR	12·1231	34·2381	89·9683	175·8939	289·3809
		ANN	12·1016	34·1701	90·0096	175·7664	289·5709
	0·3	NR	8·4535	40·9978	111·3278	194·5467	249·2325
		ANN	8·4255	40·9089	111·2261	194·6070	249·4662
	0·4	NR	7·0194	51·8276	113·1904	163·6506	297·0866
		ANN	7·0259	51·8067	113·2514	163·6979	297·3626
	0·5	NR	6·6265	61·6727	91·3187	199·8604	248·6298
		ANN	6·5904	61·6442	91·4269	199·9192	249·1638
8	0·1	NR	18·0628	31·7032	74·5124	144·1680	237·9923
		ANN	18·0555	31·7494	74·4069	144·0635	238·1725
	0·2	NR	9·0541	33·0046	89·3709	175·5386	289·2312
		ANN	9·0468	33·0075	89·4069	175·6679	289·1619
	0·3	NR	6·1637	40·3644	111 0895·	194·3543	248·2830
		ANN	6·1702	40·3744	110·6566	194·4497	248·2413
	0·4	NR	5·0819	51·4819	112·8991	162·9044	297·0487
		ANN	5·0608	51·4931	112·8521	162·8021	296·9546
	0·5	NR	4·7889	61·6727	90·4315	199·8604	247·6752
		ANN	4·8015	61·7224	90·3270	199·8819	247·4461

For the non-linear part, 2:5:5:1 architecture with two hidden layers is found to be the best suited model (Figure 7). α and η are again the input parameters and λ, the non-linear correction coefficient of the fundamental mode, is the output parameter. In all computations, the ranges of α and β are taken as $0 \leqslant \alpha \leqslant 10$ and $0 \leqslant \eta \leqslant 0{\cdot}5$ due to symmetry.

After training the algorithm using some initial training values, the algorithm is tested by contrasting some other test values obtained by conventional techniques (Newton–Raphson method for calculating natural frequencies) and by ANN. As can be seen from Table 2, results of ANN are very close to those of Newton–Raphson method with maximum 0·55% error.

The same procedure is used for finding the non-linear correction coefficient λ defined in equation (32) for the fundamental mode. The test values are contrasted using conventional techniques and ANN. Results are given in Table 3 and are again very close to each other, with maximum 0·88% error.

TABLE 3

Comparison of exact and ANN non-linear correction coefficients for the fundamental mode

α	η	λ (NR)	λ (ANN)
0·8	0·1	1·2259	1·2248
	0·2	0·9817	0·9850
	0·3	0·8297	0·8229
	0·4	0·7759	0·7795
	0·5	0·7614	0·7566
4	0·1	1·0033	1·0014
	0·2	0·5267	0·5261
	0·3	0·4410	0·4379
	0·4	0·4089	0·4124
	0·5	0·3998	0·3974
8	0·1	0·7236	0·7228
	0·2	0·3772	0·3788
	0·3	0·3196	0·3170
	0·4	0·2962	0·2988
	0·5	0·2895	0·2889

In conventional techniques, one is iterating numerically each value to assure convergence. The initial guess should be close to achieve a physical solution. However, using ANN, after half an hour of training, the tables are produced almost instantly without individual iterations. If key training values are selected well, ANN can be used efficiently to decrease drastically the computational time.

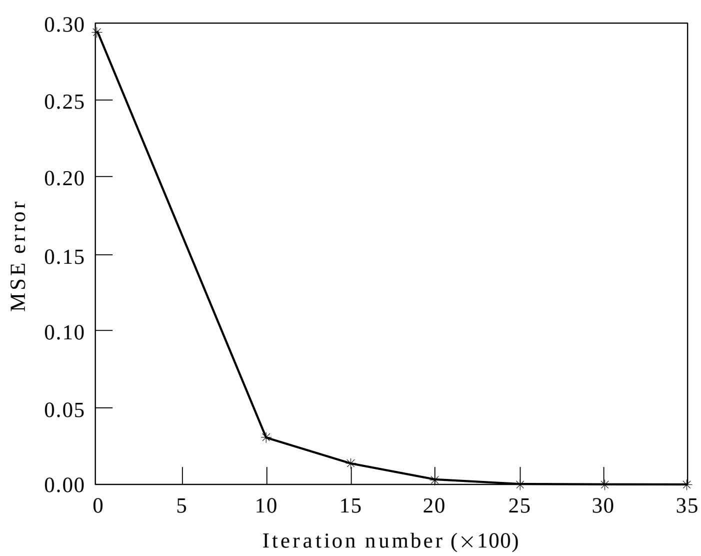

Figure 8. Iteration number versus mean square error for training natural frequencies.

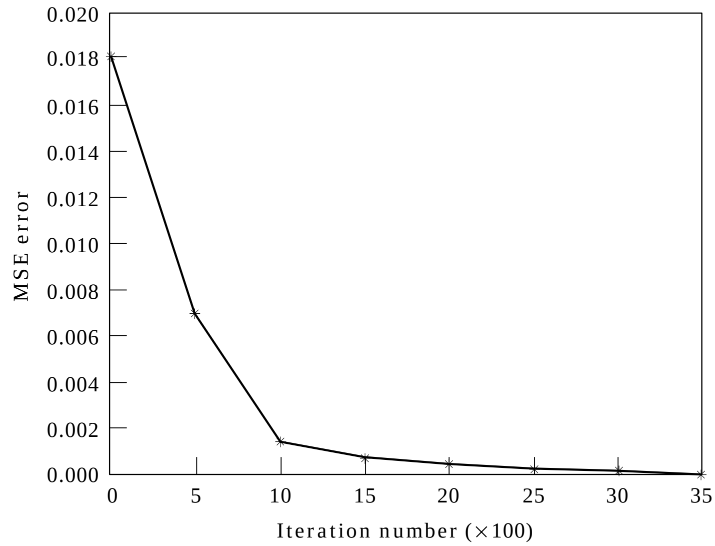

Figure 9. Iteration number versus mean square error for training non-linear correction coefficients.

In Figure 8, the mean square error versus iteration numbers of training phase are shown for the linear part. Similarly, in Figure 9, the mean square error versus iteration numbers are given for the non-linear part. From both figures it is concluded that an iteration number of 3500 reduces the error drastically. However, by taking 50 000 iterations in our analysis, the mean square error is further lowered.

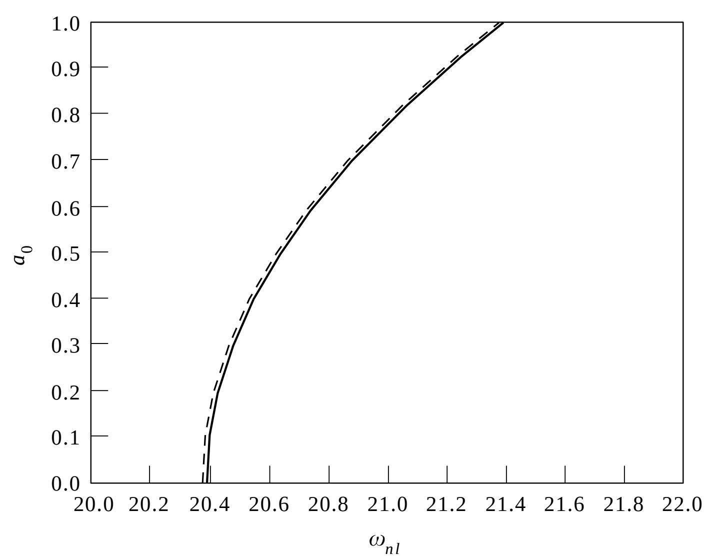

Figure 10. Comparison of non-linear frequency versus amplitude for ANN (dashed) and approximate analytical solution (solid).

Finally, Figure 10 shows a comparison of ANN (dashed) and conventional technqiues (solid) for the non-linear frequencies graphically. As can be seen, results are very close to each other.

5. CONCLUDING REMARKS

The following conclusions can be drawn from this work: (1) The beam–mass system with clamped–clamped ends is solved exactly for the mode shapes and natural frequencies. (2) An approximate non-linear analysis is carried out to find the non-linear frequencies of free vibrations and frequency–response curves of forced vibrations. (3) To increase the numerical efficiency in calculations, an ANN algorithm is adapted as a supplementary tool to the conventional techniques.

REFERENCES

1. E. Özkaya, M. Pakdemirli and H. R. Öz 1997 *Journal of Sound and Vibration* **199**, 679–696. Non-linear vibrations of a beam–mass system under different boundary conditions.
2. A. H. Nayfeh and D. T. Mook 1979 *Nonlinear Oscillations*. New York: Wiley-Interscience.
3. J. W. Hou and J. Z. Yuan 1988 *American Institute of Aeronautics and Astronautics Journal* **26**, 872–880. Calculation of eigenvalue and eigenvector derivatives for nonlinear beam vibrations.
4. P. H. McDonald 1991 *Computers and Structures* **40**, 1315–1320. Nonlinear dynamics of a beam.
5. M. Pakdemirli and A. H. Nayfeh 1994 *ASME Journal of Vibration and Acoustics* **166**, 433–438. Nonlinear vibrations of a beam–spring–mass system.
6. B. Karlik, E. Özkaya, S. Aydin and M. Pakdemirli 1998 *Computers and Structures* **69,** 339–347. Vibrations of a beam–mass systems using artificial neural networks.
7. L. W. Rehfield 1974 *American Institute of Aeronautics and Astronautics Journal* **12**, 91–93. Nonlinear flexural oscillations of shallow arches.
8. H. R. Öz, M. Pakdemirli, E. Özkaya and M. Yilmaz 1998 *Journal of Sound and Vibration* **212**, 295–309. Non-linear vibrations of a slightly curved beam resting on a non-linear elastic foundation.
9. K. H. Low, T. M. Lin and G. B. Chai 1993 *Computers and Structures* **48**, 1157–1162. Experimental and analytical investigations of vibration frequencies for center-loaded beams.
10. G. B. Chai, K. H. Low and T. M. Lin 1995 *Journal of Sound and Vibration* **181**, 727–736. Tension effects on the natural frequencies of center-loaded clamped beams.
11. K. H. Low 1997 *Journal of Sound and Vibration* **201**, 528–533. Closed form formulas for fundamental vibration frequency for beams under off-center load.
12. K. H. Low 1997 *Journal of Sound and Vibration* **207**, 284–286. Comments on "Non-linear vibrations of a beam–mass system under different boundary conditions".
13. K. H. Low 1997 *Journal of Sound and Vibration* **207**, 132–135. Further note on closed-form formulas for fundamental vibration frequency of beams under off-center load.
14. M. A. De Rosa, C. Franciosi and J. Maurizi 1996 *Computers and Structures* **58**, 1145–1159. On the dynamic behavior of slender beams with elastic ends carrying a concentrated mass.